

Three-Dimensional Architectures Incorporating Stereoregular Donor–Acceptor Stacks

Dennis Cao,^[a, b] Michal Juríček,^[a] Zachary J. Brown,^[a] Andrew C.-H. Sue,^[a]
Zhichang Liu,^[a] Juying Lei,^[a] Anthea K. Blackburn,^[a] Sergio Grunder,^[a]
Amy A. Sarjeant,^[a] Ali Coskun,^[a, b] Cheng Wang,^[a, c] Omar K. Farha,^[a]
Joseph T. Hupp,^[a] and J. Fraser Stoddart*^[a, b]

Dedicated to the memory of Christian G. Claessens

Abstract: We report the synthesis of two [2]catenane-containing struts that are composed of a tetracationic cyclophane (TC⁴⁺) encircling a 1,5-dioxy-naphthalene (DNP)-based crown ether, which bears two terphenylene arms. The TC⁴⁺ rings comprise either 1) two bipyridinium (BIPY²⁺) units or 2) a BIPY²⁺ and a diazapyrenium (DAP²⁺) unit. These degenerate and nondegenerate catenanes were reacted in the presence of Cu(NO₃)₂·2.5H₂O to yield Cu-paddlewheel-based MOF-1050 and MOF-1051. The solid-state structures of these MOFs reveal that the metal clusters serve to join the heptaphenylene struts into grid-like 2D networks. These 2D sheets are then held together

by infinite donor–acceptor stacks involving the [2]catenanes to produce interpenetrated 3D architectures. As a consequence of the planar chirality associated with both the DNP and hydroquinone (HQ) units present in the crown ether, each catenane can exist as four stereoisomers. In the case of the nondegenerate (bistable) catenane, the situation is further complicated by the presence of translational isomers. Upon crystallization, however, only two of the four possible stereoisomers—namely, the enantiomeric *RR* and *SS* forms—are observed in the crystals. An additional element of conformational selectivity is present in MOF-1051 as a consequence of the substitution of one of the BIPY²⁺ units by a DAP²⁺ unit: only the translational isomer in which the DAP²⁺ unit is encircled by the crown ether is observed. The overall topologies of MOF-1050 and MOF-1051, and the selective formation of stereoisomers and translational isomers during the kinetically driven crystallization, provide evidence that weak noncovalent bonding interactions play a significant role in the assembly of these extended (super)structures.

Keywords: catenanes • molecular recognition • pi–pi stacking • self-assembly • stereochemistry

Introduction

Substrate-binding receptors^[1] (SBRs) and mechanically interlocked molecules^[2] (MIMs) have been incorporated into

well-defined, extended architectures^[3] of metal–organic frameworks^[4] (MOFs) and nanoporous coordination polymers^[5] (NCPs) in a quest to marry^[6] the dynamics of SBRs and MIMs with the robustness of MOFs and NCPs. The organic struts located between the metal secondary binding units (SBUs) in MOFs serve as ideal platforms for the insertion of SBRs and MIMs into the highly ordered three-dimensional (3D) scaffold of a MOF or an NCP.

We have shown^[7] previously that rigid dicarboxylate struts, containing degenerate $\pi\cdots\pi$ donor–acceptor (DA) [2]catenanes, form—depending on the length of the struts—either 2D or 3D Cu-based MOF-1011^[7a] or MOF-1030,^[7b] respectively, in which the SBUs consist of a single Cu^I ion. It transpires, however, that some of the acetylenic linkers used to extend the backbone of the struts also coordinate to the SBUs, resulting in a mode of binding in which each dicarboxylate strut is associated with three separate metal ions, two with the carboxylates and one in which Cu^I ions coordinate to an acetylenic linker in an η^2 fashion. The catenanes present in MOF-1011 form infinite DA stacks, while in MOF-1030, pairs of catenanes, which are associated through $\pi\cdots\pi$ stacking of their hydroquinone (HQ) units, are sand-

[a] D. Cao, Dr. M. Juríček, Z. J. Brown, Dr. A. C.-H. Sue, Dr. Z. Liu, J. Lei, A. K. Blackburn, Dr. S. Grunder, Dr. A. A. Sarjeant, Prof. A. Coskun, Prof. C. Wang, Prof. O. K. Farha, Prof. J. T. Hupp, Prof. J. F. Stoddart
Department of Chemistry, Northwestern University
2145 Sheridan Road, Evanston, Illinois 60208 (USA)
Fax: (+1)847-491-1009
E-mail: stoddart@northwestern.edu

[b] D. Cao, Prof. A. Coskun, Prof. J. F. Stoddart
NanoCentury KAIST Institute and Graduate School of EEWS
Korea Advanced Institute of Science and Technology (KAIST)
373-1 Guseong Dong, Yuseong Gu
Daejeon 305-701 (Republic of Korea)

[c] Prof. C. Wang
College of Chemistry and Molecular Sciences
Wuhan University, Wuhan 430072 (P. R. China)

Supporting information for this article is available on the WWW under <http://dx.doi.org/10.1002/chem.201300762>.

wiched between phenylene/acetylene regions on adjacent struts. In order to remove the complications involving η^2 binding to triple bonds, struts free of reactive acetylenic linkers are required to act as the building blocks. In response to this requirement, we report herein 1) the incorporation of the [2]catenane-containing heptaphenylene struts,^[8] **1⁴⁺** and **2⁴⁺** (Figure 1), into Cu paddlewheel-based^[9] MOFs

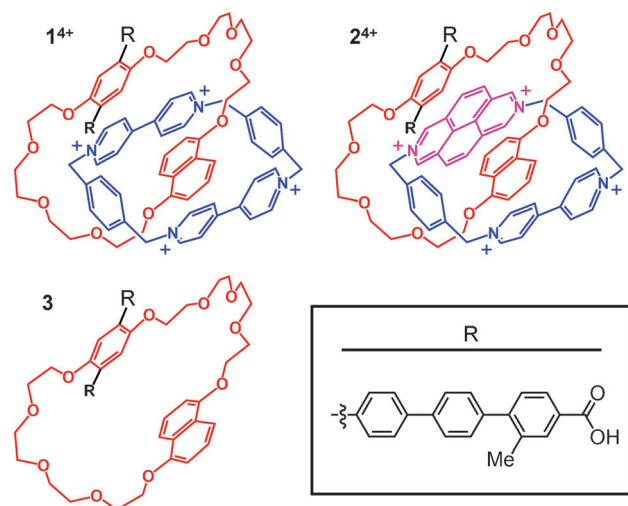


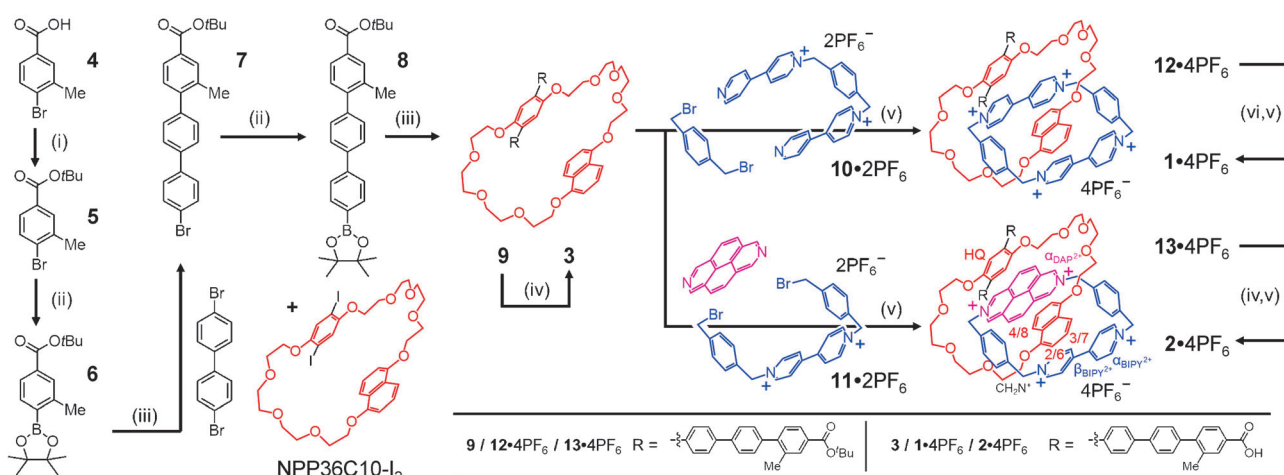
Figure 1. Structural formulas of the *RR* forms of the [2]catenanes **1⁴⁺** and **2⁴⁺**, and the crown ether **3**. All three molecules bear heptaphenylene backbones terminated by carboxylic acid groups.

in which 2) separate, alternating, 2D layers in the solid state are linked by means of DA $\pi \cdots \pi$ stacking interactions^[10] in 3) a stereoregular manner, which 4) selects for the dual planar chirality present in the catenanes in 5) the form of syndiotactic-like arrays^[11] in order to create stacks in which *RR* and *SS* enantiomers alternate with each other.

Results and Discussion

The synthesis of **1·4PF₆** and **2·4PF₆**, as well as the free [36]crown-10-containing heptaphenylene strut **3**, were achieved (Scheme 1) by a series of Miyaura borylations^[12] and Suzuki cross-couplings.^[13] The methyl groups on the terminal phenylene units are extremely important, since they confer enough solubility to render^[8] every neutral precursor soluble in the chlorinated solvents employed in their workup. Commercially available 4-bromo-3-methylbenzoic acid (**4**) was esterified with *t*BuOH to yield the benzoic ester **5**. Subsequent borylation of **5** by treatment with KOAc, bis(pinacolato)diboron, and [Pd(dppf)Cl₂] in (CH₃)₂SO furnished the boronic ester **6** in 97% yield. Reaction of **6** with a threefold excess of 4,4'-dibromobiphenyl in the presence of [Pd(dppf)Cl₂] and CsF in a *p*-dioxane/H₂O (3:1 v/v) solvent mixture yielded the terphenylene **7** in 24% yield. This low yield is a consequence of a side reaction in which both bromides on a single 4,4'-dibromobiphenyl molecule react with **6**, resulting in the formation of an unwanted tetraphenylene diester. This byproduct, along with any excess of unreacted 4,4'-dibromobiphenyl, can be separated easily from the desired product—namely **7**—by column chromatography. Borylation at the remaining bromine site in **7** afforded the terphenylene boronic ester **8**, which was then cross-coupled with a macrocyclic polyether, namely NPP36C10-I₂,^[14] to yield the key intermediate **9** in 64% yield. The hydroquinone (HQ) unit in the macrocyclic polyether bears two terphenylene units *para* to each other such that, in combination with the HQ ring, they constitute a hepta(*p*-phenylene) backbone. Deprotection of the *tert*-butyl ester groups by treatment with a mixture of trifluoroacetic acid (TFA)/CH₃CN (1:1 v/v) afforded the macrocyclic polyether-containing diacid **3** in 96% yield.

The reaction of dicationic intermediate^[15] **10·2PF₆** with 1,4-bis(bromomethyl)benzene in the presence of **9** for three



Scheme 1. Synthesis of the [2]catenanes **1·4PF₆** and **2·4PF₆** and the macrocyclic polyether **3**. Reagents and conditions: i) DMAP, *t*BuOH, THF, reflux. ii) [Pd(dppf)Cl₂], (Bpin)₂, (CH₃)₂SO, KOAc, 80 °C. iii) [Pd(dppf)Cl₂], *p*-dioxane/H₂O (3:1 v/v), CsF, reflux. iv) TFA/CH₃CN. v) NH₄PF₆/H₂O. vi) HCl/CH₃CN.

days under ambient conditions afforded the [2]catenane **12**·4PF₆ in 90% yield after purification by column chromatography. De-esterification was achieved by treating **12**·4PF₆ with a solution of HCl in CH₃CN (3:4 v/v). The purple precipitate that formed during the reaction was collected and redissolved in H₂O with the assistance of a small amount of CH₃OH. Addition of NH₄PF₆ to the aqueous solution precipitated a purple solid which was shown to be the [2]catenane **1**·4PF₆. The [2]catenane **2**·4PF₆ was synthesized following a templation protocol similar to that employed in the synthesis of **1**·4PF₆. The formation of the catenane was achieved by reacting 2,7-diazapyrene (**14**)—which was synthesized^[16] following a literature protocol (see the Supporting Information)—with the dicationic intermediate^[17] **11**·2PF₆ in the presence of the macrocyclic polyether **9** as a template. Column chromatography of the crude product yielded the [2]catenane **13**·4PF₆, which was then converted into **2**·4PF₆ by treatment with a mixture of TFA and CH₃CN (1:1 v/v). Counterion exchange of the crude product furnished the [2]catenane **2**·4PF₆ as a red solid in 76% yield over two steps.

Both the HQ unit, which is located in the middle of the heptaphenylene strut and the 1,5-dioxynaphthalene (DNP) unit in the [36]crown-10 exhibit^[14] planar chirality (Figure 2). The assignment of absolute configuration of molecules with chiral planes involves,^[18] in the first instance, the selection of an out-of-plane “pilot atom” that is directly attached to an atom which is located within the plane of the planar chiral element in question. In the case of **1**·4PF₆ and **2**·4PF₆, any of the carbon atoms—highlighted by green circles in Figure 2—attached to the HQ and DNP unit oxygen atoms will suffice. The next three atoms encountered, while counting within the plane in question, are chosen by precedence according to CIP rules,^[19] as shown by a, b, and c in Figure 2. When viewed from the pilot atom, if the a–b–c array is clockwise, then the absolute configuration is *R*, and if the array is counterclockwise, then the absolute configuration is *S*. In the case of the [2]catenane strut illustrated in

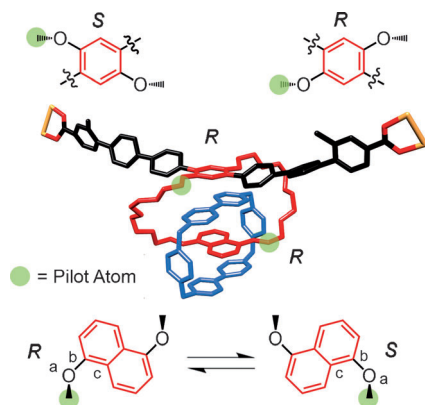


Figure 2. Assignment of *R* configurations to both the HQ and DNP units in one *RR* of the two enantiomeric [2]catenanes located within MOF-1050. The green circles highlight the atoms which are utilized as “pilot atoms” to conduct the assignment of planar chirality.

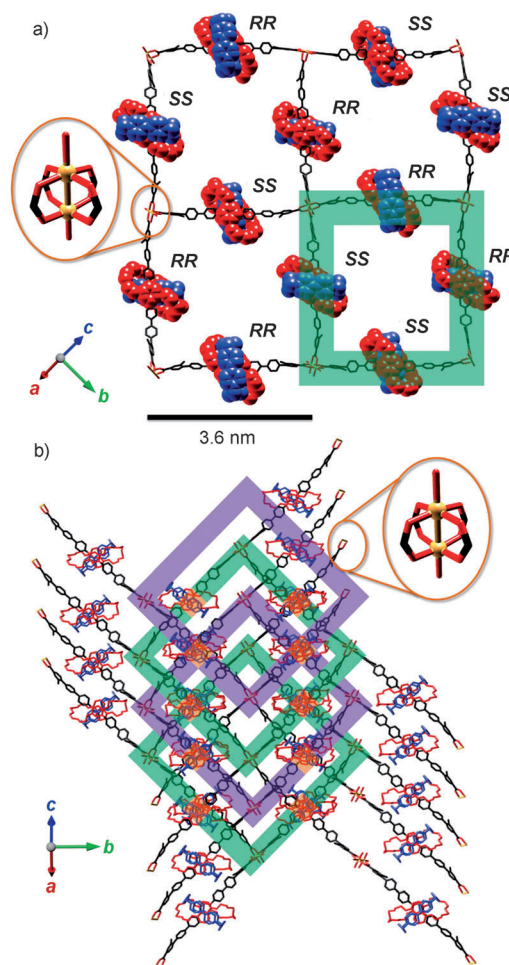


Figure 3. a) A single layer of MOF-1050 as viewed from the [102] direction. The planar chiralities of the catenane sub-structures are assigned to the descriptors *RR* and *SS*. The TC⁴⁺ rings and the crown ethers are illustrated in space-filling format while other atoms are portrayed in a stick representation. b) Four stacked layers in the stick representation. The DA stacks of catenanes and the layers are packed along the [102] axis. Individual layers are highlighted by pale green and pale purple boxes. Layers associated by DA interactions are of the same color and stacks of catenanes are highlighted by orange squares. Inset: Cu paddlewheels. Cu = gold/crown ethers = red/TC⁴⁺ = blue/organic struts = black. All hydrogen atoms have been omitted for the sake of clarity.

Figure 2, both the HQ and DNP units have *R* configurations. The stereoisomers associated with the HQ unit cannot undergo inversion simply because the overall length of the strut is more than sufficient to prevent the passage of a terphenylene unit through the middle of the [36]crown-10. On the other hand, the DNP unit in the macrocyclic polyether in **3** can undergo inversion of its planar chirality by a simple pedaling motion: although this motion will be impaired in the [2]catenanes **1**⁴⁺ and **2**⁴⁺, it can still happen^[20] as a result of the DNP units leaving the cavity of the tetracationic cyclophane (TC⁴⁺) momentarily. In other words, in solution, the *RR* and *SS* enantiomers of **1**⁴⁺, **2**⁴⁺, and **3** are, in principle at least, in equilibrium with their *RS* and *SR* enantiomeric pair of diastereoisomers, respectively. Additionally, in the case of **2**⁴⁺ in which the mechanically interlocked

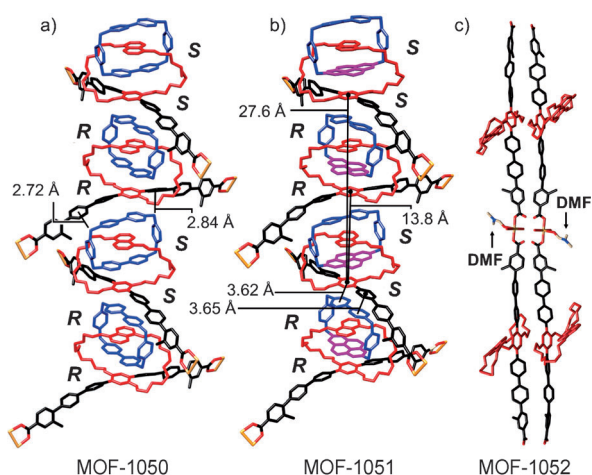


Figure 4. DA stacks of four catenanes in a) MOF-1050 and b) MOF-1051. C–H \cdots π and $\pi\cdots\pi$ interaction distances are denoted in a) and b), respectively. In both MOFs, the struts are bent around the adjacent TC⁴⁺ rings. The backbones of neighboring struts within a stack are offset by 86° from each other. The planes of chirality associated with the catenane substructures are assigned to the descriptors *R* and *S*. c) Two adjacent 1D chains of macrocyclic polyether-containing struts in MOF-1052. A single Cu^{II} ion links each chain together. Cu = gold/crown ethers = red/TC⁴⁺ = blue and magenta/organic struts = black. In c), a DMF molecule (white and blue) is coordinated to each Cu^{II} ion. All hydrogen atoms have been omitted for the sake of clarity.

TC⁴⁺ incorporates both bipyridinium (BIPY²⁺) and 2,7-diazapyrenium (DAP²⁺) units, two translational isomers are observed^[21] in the approximate ratio of 3:1 in favor of the isomer where the [36]crown-10 encircles the DAP²⁺.

Single crystals of [Cu₂(1)₂(H₂O)₂] (MOF-1050) and [Cu₂(2)₂(H₂O)₂] (MOF-1051) were obtained by heating (80–85 °C) solutions of **1**·4PF₆ and **2**·4PF₆, respectively, and an excess^[22] of Cu(NO₃)₂·2.5H₂O in mixtures of dimethylformamide (DMF) or diethylformamide (DEF) in aqueous EtOH—essentially the same conditions as those employed^[7] to produce MOF-1011 and MOF-1030. X-ray crystallography carried out on the single crystals reveals^[23] (Figures 3 and 4) that MOF-1050^[24] and MOF-1051^[25] are isostructural, consisting of a 2D network (Figure 3) in which the struts are joined together by copper paddlewheel^[9] SBUs. Prior to the formation of MOF-1050, a total of four stereoisomers—*RR*, *RS*, *SR*, and *SS*, in which the first and second descriptors refer to that of the HQ and DNP units, respectively—of the catenanes are present^[7b] in the crystallization solution. More often than not,^[26] DA catenanes crystallize to form continuous $\pi\cdots\pi$ stacks in the solid state with the planar chirality associated with any individual stack being invariably offset by a neighboring $\pi\cdots\pi$ stack adopting the opposite elements of planar chirality. It is worth noting that, upon formation of the extended structures, only *one* of the diastereoisomeric pairs of enantiomers is present—namely, the *RR* and *SS* forms—indicating that diastereoselection processes are taking place during the crystallization of MOF-1050 and MOF-1051. This diastereoselection suggests that the intermolecular $\pi\cdots\pi$ stacking of catenanes with each other plays

a major role in the assembly of the crystalline MOF despite the fact that these interactions are considerably weaker than the coordinative bonds which bind the organic struts to the metal joints.

Moreover, in MOF-1051, the DAP²⁺ units reside exclusively inside the cavity of the macrocyclic polyether, indicating that a co-conformational selection process is taking place during the crystallization process in addition to the diastereoselective ones. This outcome is in stark contrast with solution-state observations (Figure 5)—namely, that the two different translational isomers of **2**⁴⁺ exist in a roughly 3:1 ratio in favor of encirclement of the DAP²⁺ unit. A close inspection of the ¹H NMR spectrum (Figure 5) of **2**⁴⁺ reveals peaks corresponding to the two different translational isomers. The minor peaks can be assigned to the translational isomer in which the BIPY²⁺ unit is encircled by the crown ether, while the other more intense peaks correspond to the translational isomer in which the TC⁴⁺ encircles the DAP²⁺ unit within the crown ether. Integration of the major and minor peaks indicates that the translational isomers exist in a roughly 3:1 ratio in favor of the one involving encirclement of the DAP²⁺ unit in the TC⁴⁺ by the crown ether.

The catenanes in the alternating layers in these two metal–organic frameworks exhibit (Figure 4a,b) extended DA stacking interactions with each other, resulting in two separate sets of layers, which are highlighted in purple and green in Figure 3b. When viewed down the [102] direction, each 2D layer is offset slightly—that is, staggered with respect to those immediately above and below it. Every layer, be it purple or green, is in register—that is, eclipsed—with those either four above or four below it. Within any particular layer—purple or green—the catenanes are arranged in a half-up/half-down manner, comprising *RR* and *SS* forms in equal numbers inside each square, for which the sides are approximately 3.6 nm in length. Analysis of these alternating purple and green (Figure 4a) layers reveals that within any one layer, the catenanes exhibit one—either *RR* or *SS*—

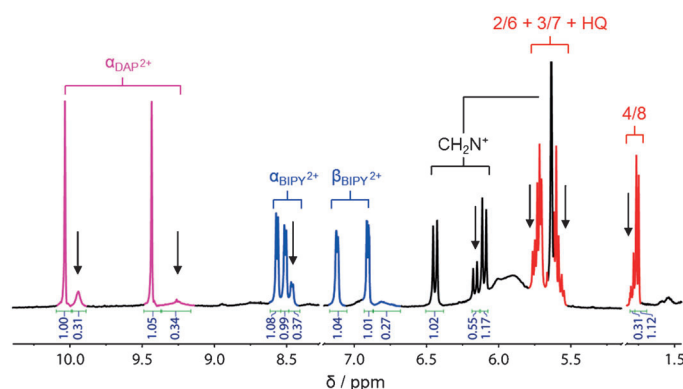


Figure 5. ¹H NMR spectrum (CD₃CN, 500 MHz, 298 K) of **2**·4PF₆. The resonances are assigned according to the labels in Figure 1. Peaks corresponding to the minor isomer—namely, the one in which the bipyridinium unit is encircled by the macrocyclic polyether—are indicated by black arrows. Parts of the spectrum have been omitted for the sake of clarity.

absolute configuration along one diagonal in which the catenanes alternate up-down-up-down, while along the orthogonal diagonal, in which the catenanes are either all up or all down, the absolute configurations of the catenanes alternate between *RR* and *SS* along the diagonal. The alternating purple and green layers are conjugated (Figure 6) in a syn-

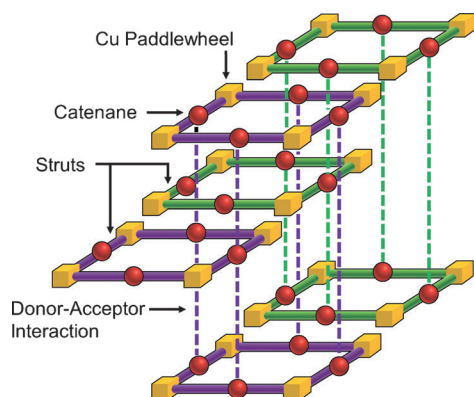


Figure 6. Graphical representation of the MOF-1050 topology. DA interactions hold the 2D MOF layers together. The layers are organized such that every other layer—that is purple or green—experiences DA interactions with each other. The purple layers stack together and the green layers stack together.

diotactic-like manner^[11] by $\pi\cdots\pi$ stacking interactions involving DA catenanes and their associated struts, such that the *RR* forms alternate in the stacks with the *SS* forms. MOF-1050 is reminiscent of “pillared” MOFs^[27] in which bispyridyl ligands coordinated to the metal paddlewheel SBUs are used to create separation between 2D sheets. In the [2]catenane-containing MOFs, however, the DA stacks take the place of the bispyridyl ligands and extend the connectivity of the organic struts beyond the second dimension into the third one. The purple and green layers and their associated DA stacks therefore constitute an interpenetrated 3D architecture in which noncovalent bonding assumes the role normally served by covalent and coordination bonds.

The methyl groups on the two terminal phenyl groups act as steric barriers which induce a torsional twist of 50 and 102° with respect to their contiguous aromatic rings. On the other hand, the torsional angles between the remaining phenylene rings and the central HQ unit vary only by between 22 and 28°. The heptaphenylene backbones of the struts in MOF-1050 and MOF-1051 are bent^[28] by approximately 24°, and the struts themselves are lined up almost perfectly (6° displacement) with the BIPY²⁺ unit occupying the alongside position in the neighboring catenane. The centroid-to-centroid distance from an HQ unit to the nearest pyridinium ring in an adjacent [2]catenane (Figure 4b) is 3.62 Å. Similarly, the other pyridinium unit that is not encircled by the crown ether is within $\pi\cdots\pi$ stacking distance of one of the phenylene rings attached to the HQ unit, with a centroid-to-centroid distance (Figure 4b) of 3.65 Å. Furthermore, the methylene protons in the TC⁴⁺ ring are engaged in C–H $\cdots\pi$

interactions with the closest phenylene rings and have distances (Figure 4a) typically of 2.72 and 2.84 Å between the plane of the phenylene ring and the hydrogen atoms. These interstrut distances suggest that $\pi\cdots\pi$ and C–H $\cdots\pi$ interactions of the BIPY²⁺ and CH₂N⁺ units with the adjacent phenylene rings provide the driving force that leads to the bent nature of the strut backbones and their orientations with respect to the adjacent TC⁴⁺ rings. A consequence of the alignment between the TC⁴⁺ rings and the oligophenylene backbones is that the alternating struts and TC⁴⁺ rings are arranged at almost (ca. 86°) right angles to each other. The crossed alignment of the cyclophanes is rarely observed^[29] in TC⁴⁺-containing [2]catenanes. The distance between adjacent HQ centroids of *RR* and *SS* forms within a DA stack is 13.8 Å, while the distance between [2]catenanes of the same stereochemistry is 27.6 Å. These distances (Figure 4b) correspond^[10] to a typical $\pi\cdots\pi$ stacking distance of 3.5 Å between aromatic units. The net result is that the $\pi\cdots\pi$ stacking interactions between alternating layers is optimal, suggesting that DA self-assembly contributes to the formation of the interpenetrated extended (super)structures that constitute MOF-1050 and MOF-1051. Despite this interpenetration, there are channels (Figure 7) running along the *a* and *c* axes in MOF-1050 and MOF-1051 that constitute in large measure the solvent-accessible voids,^[30] which represent 57% of the crystal. The channels along the *a* axis are 19.4 Å at their widest, while the smaller channels which run along the *c* axis measure about 7.7 Å across. By way of com-

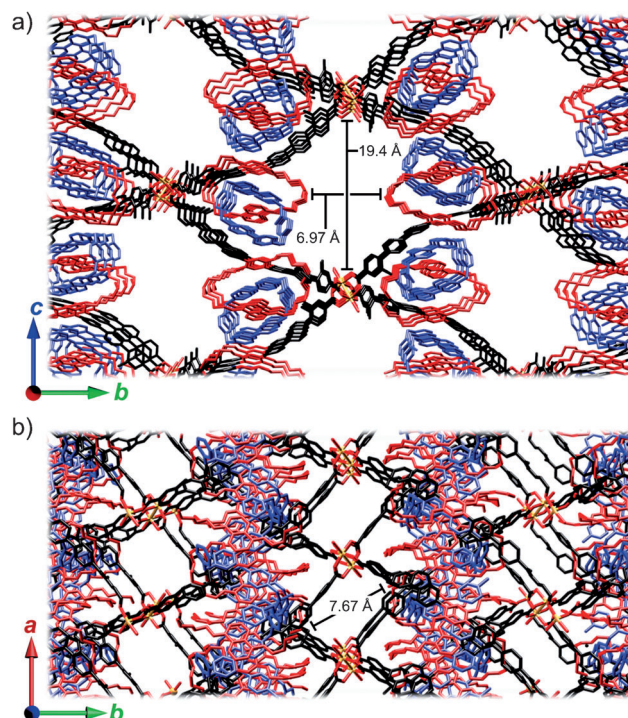


Figure 7. The channels present in MOF-1050 as viewed along the a) *a* and b) *c* axes. In both a) and b), Cu=gold/crown ethers=red/TC⁴⁺=blue/organic struts=black. All hydrogen atoms have been omitted for the sake of clarity.

parison, the unit cell volumes of MOF-1011 and MOF-1030 are composed^[7a,b] of only 0.2 and 35% solvent-accessible voids, respectively.

The importance of noncovalent bonding interactions in the formation of these MOFs is supported additionally by the results of a control experiment in which the DA catenanes in **1**⁴⁺ and **2**⁴⁺ have their tetracationic cyclophanes removed to produce a strut **3**, which incorporates only the [36]crown-10. When **3** and Cu(NO₃)₂·2.5H₂O were heated to 60 °C in a mixture of DMF and aqueous EtOH, crystals of [Cu(**3**)(H₂O)₂(dmf)] (MOF-1052) were obtained. X-ray crystallography reveals^[23,31] that the organic struts are linked together by a single Cu^{II} ion so as to form 1D polymer chains (Figure 4c) that are packed tightly together. The removal of the enthalpic contributions provided by the DA stacks associated with the catenanes in MOF-1050 and MOF-1051 results in a dramatic change in the solid-state (super)structure—that is, it would seem that noncovalent bonding interactions are driving the formation of MOF-1050 and MOF-1051.

Conclusion

The cumulative effect of noncovalent bonding interactions in the shape of $\pi\cdots\pi$ stacks provided by suitably located donor–acceptor catenanes can aid and abet the formation of robust extended structures such that the two elements of planar chirality associated with the stacked catenanes undergo self-sorting into only one repeating enantiomer pair of diastereoisomers. These observations demonstrate that it is possible to call upon the tenets of supramolecular^[32] and coordination chemistry^[33] to construct rigid, porous three-dimensional architectures that could play host to artificial molecular switches^[34] and machines^[35] one day, provided the mechanically interlocked molecules are capable of undergoing mechanostereochemical^[36] dynamic motions in the solid state.

Experimental Section

General information: Solvents were deoxygenated by passing Ar gas through the solution for 30 min. Compound **4** and reagents were purchased from Sigma–Aldrich and used as received, unless otherwise noted. All reactions were performed under a N₂ atmosphere and in dry solvents, unless otherwise stated. All cross-coupling reactions were carried out in deoxygenated solvents under N₂ using the Schlenk technique. Compounds **5**,^[37] NPP36C10-I₂,^[14] **10**-2PF₆,^[15] and **11**-2PF₆^[17] were all prepared following literature procedures. Analytical thin-layer chromatography (TLC) was performed on aluminum sheets precoated with silica gel 60-F254 (Merck 5554). Column chromatography was carried out using silica gel 60F (Silicycle 230–400 mesh). Nuclear magnetic resonance (NMR) spectra were recorded at 298 K on a Bruker Avance III 500 spectrometer, with a working frequency of 500 MHz for ¹H and 125 MHz for ¹³C. Chemical shifts are listed in ppm on the δ scale and coupling constants are recorded in Hertz (Hz). Deuterated solvents for NMR spectroscopic analyses were used as received. Chemical shifts are reported in δ relative to the signals corresponding to the residual non-deuterated solvents (CDCl₃: δ_{H} 7.26 ppm, δ_{C} 77.16 ppm, CD₃CN: δ_{H} 1.94 ppm, δ_{C}

1.32 ppm, CD₃SOCD₃: δ_{H} 2.50 ppm, δ_{C} 39.52 ppm). The following abbreviations are used to explain the multiplicities: s, singlet; d, doublet; t, triplet; br, broad peaks; m, multiplet or overlapping peaks. AA'BB' and AA'XX' are used to denote *para*-phenylene and 4-substituted pyridinium protons. The NMR spectra were processed using the MestReNova 7.1 chemistry software suite. High-resolution electrospray ionization (HR ESI) mass spectra were measured on Agilent 6210 LC-TOF with Agilent 1200 HPLC introduction.

Synthesis of compound 6: A mixture of *tert*-butyl ester **5**^[37] (12.5 g, 46.0 mmol), bis(pinacolato)diboron (12.9 g, 50.8 mmol), [Pd(dppf)Cl₂] (1.9 g, 2.3 mmol), KOAc (13.6 g, 139 mmol), and (CH₃)₂SO (200 mL) was heated at 80 °C under N₂ for 10 h. The reaction mixture was then cooled to RT, diluted with CH₂Cl₂, and washed copiously with H₂O to remove (CH₃)₂SO and inorganic salts. The organic layer was dried (MgSO₄), filtered, and the solvent evaporated. The residue was then purified by column chromatography on silica gel using EtOAc/hexanes (1:4 v/v) to yield **6** (14.3 g, 97%) as an off-white solid. ¹H NMR (CDCl₃, 500 MHz, 298 K): δ = 7.72–7.78 (m, 3H), 2.56 (s, 3H), 1.59 (s, 9H), 1.35 ppm (s, 12H); ¹³C NMR (CDCl₃, 125 MHz, 298 K): δ = 166.1, 144.8, 135.7, 133.8, 130.4, 125.5, 83.9, 83.7, 81.1, 28.4, 28.3, 25.2, 25.0, 22.3 ppm; HR MS (ESI): *m/z* calcd for C₁₈H₂₇BO₄: 317.2040 [*M*]⁺; found: 317.2039.

Synthesis of compound 7: A mixture of boronic ester **6** (12 g, 38 mmol), 4,4'-dibromobiphenyl (14.7 g, 113 mmol), [Pd(dppf)Cl₂] (1.5 g, 1.8 mmol), CsF (17.2 g, 113 mmol), and a 3:1 (v/v) mixture of *p*-dioxane/H₂O (1300 mL) was heated under reflux under N₂ for 16 h. After cooling to RT, the reaction mixture was filtered. The filtrate was diluted with CH₂Cl₂ and washed with H₂O and brine. The organic layers were combined, dried (MgSO₄), filtered, and the solvent evaporated. The residue was purified by column chromatography on silica gel using hexanes to elute the excess of 4,4'-dibromobiphenyl and hexanes/CH₂Cl₂ (7:1 v/v) to obtain **7** (5.4 g, 24%) as a white solid. ¹H NMR (CDCl₃, 500 MHz, 298 K): δ = 7.92 (s, 1H), 7.87 (dd, *J* = 8.0, 1.7 Hz, 1H), 7.63 (AA'BB', *J* = 7.0 Hz, 2H), 7.60 (AA'BB', *J* = 7.0 Hz, 2H), 7.52 (AA'XX', *J* = 8.2 Hz, 2H), 7.40 (AA'XX', *J* = 8.2 Hz, 2H), 7.32 (d, *J* = 7.8 Hz, 1H), 2.36 (s, 3H), 1.63 ppm (s, 9H); ¹³C NMR (CDCl₃, 125 MHz, 298 K): δ = 166.0, 145.6, 140.6, 140.6, 139.7, 139.0, 135.6, 132.0, 131.5, 131.0, 129.9, 129.7, 128.8, 127.0, 126.9, 121.8, 81.1, 28.4, 20.7 ppm; HR MS (ESI): *m/z* calcd for C₂₄H₂₃BrO₂: 445.0771 [*M*+Na]⁺; found: 445.0788.

Synthesis of compound 8: A mixture of *tert*-butyl ester **7** (5.3 g, 13 mmol), bis(pinacolato)diboron (3.6 g, 14 mmol), [Pd(dppf)Cl₂] (0.5 g, 0.6 mmol), KOAc (3.8 g, 39 mmol), and (CH₃)₂SO (100 mL) was heated at 80 °C under N₂ for 10 h. The reaction mixture was then cooled to RT, diluted with CH₂Cl₂, and washed copiously with H₂O to remove (CH₃)₂SO and inorganic salts. The organic layer was dried (MgSO₄), filtered, and solvent evaporated. The residue was then purified by column chromatography on silica gel using CH₂Cl₂/hexanes (1:4 v/v) to yield **8** (4.15 g, 70%) as a white solid. ¹H NMR (CDCl₃, 500 MHz, 298 K): δ = 7.94 (s, 1H), 7.93 (AA'BB', *J* = 8.0 Hz, 2H), 7.90 (AA'BB', *J* = 8.0 Hz, 1H), 7.70 (AA'XX', *J* = 8.6 Hz, 2H), 7.68 (AA'XX', *J* = 8.6 Hz, 2H), 7.41 (AA'BB', *J* = 8.0 Hz, 2H), 7.33 (AA'BB', *J* = 8.0 Hz, 1H), 2.38 (s, 3H), 1.63 (s, 9H), 1.38 ppm (s, 12H); ¹³C NMR (CDCl₃, 125 MHz, 298 K): δ = 165.9, 145.7, 143.4, 140.5, 140.0, 135.6, 135.4, 131.5, 130.9, 129.9, 129.6, 127.1, 127.0, 126.5, 84.0, 81.0, 28.3, 25.0, 20.7 ppm; HR MS (EI): *m/z* calcd for C₃₀H₃₅BO₄: 492.2548 [*M*+Na]⁺; found: 492.2557.

Synthesis of compound 9: A mixture of boronic ester **8** (1.0 g, 2.1 mmol), NPP36C10-I₂^[14] (0.81 g, 1.0 mmol), [Pd(dppf)Cl₂] (80 mg, 0.10 mmol), CsF (0.88 mg, 5.8 mmol), and a 3:1 (v/v) mixture of *p*-dioxane/H₂O (150 mL) was heated under reflux under N₂ for 16 h. After cooling to RT, the reaction mixture was filtered. The filtrate was diluted with CH₂Cl₂ and washed with H₂O and brine. The organic layers were combined, dried (MgSO₄), filtered, and evaporated. The residue was purified by column chromatography on silica gel using CH₂Cl₂ then EtOAc/CH₂Cl₂ (1:9 v/v) to yield **9** (780 mg, 64%) as an off-white solid. Although **9** exists presumably as a mixture of four stereoisomers, the signals for the stereoisomers overlap within the resolution limits of both ¹H and ¹³C NMR spectroscopic techniques. ¹H NMR (CDCl₃, 500 MHz, 298 K): δ = 7.94 (s, 2H), 7.89 (dd, *J* = 8.0, 1.8 Hz, 2H), 7.79 (AA'XX', *J* = 8.4 Hz, 2H), 7.72 (AA'BB', 8.0 Hz, 4H), 7.70 (AA'BB', 8.0 Hz, 4H), 7.67

(AA'XX', $J=8.4$ Hz, 4H), 7.43 (d, $J=8.2$ Hz, 4H), 7.36 (d, $J=7.9$ Hz, 2H) 7.19 (dd, $J=8.0, 8.0$ Hz, 2H), 6.97 (s, 2H), 6.63 (d, $J=7.6$ Hz, 2H), 5.30 (s, 2H), 4.16–4.07 (m, 4H), 4.05–3.95 (m, 4H), 3.93–3.88 (m, 4H), 3.78–3.57 (m, 20H), 2.40 (s, 6H), 1.63 ppm (s, 18H); ^{13}C NMR (CDCl_3 , 125 MHz, 298 K): $\delta=166.0, 154.3, 150.4, 145.8, 140.1, 140.0, 139.2, 137.4, 135.6, 131.5, 130.1, 130.3, 130.2, 129.9, 129.6, 127.0, 126.9, 126.8, 126.7, 125.1, 116.1, 114.6, 105.7, 81.1, 71.1, 71.0, 70.9, 70.9, 69.9, 69.8, 69.2, 68.0, 53.6, 28.4, 20.7$ ppm; HR MS (ESI): m/z calcd for $\text{C}_{80}\text{H}_{86}\text{O}_{14}$: 1288.6356 $[M+\text{NH}_4]^+$; found: 1288.6366.

Synthesis of compound 3: A mixture of **9** (369 mg, 0.290 mmol), TFA (20 mL), and CH_3CN (20 mL) was stirred at room temperature for 19 h before a white precipitate, which formed during this period, was filtered off, washed with H_2O , and dried in air to afford the pure product **3** (324 mg, 96%) as a white solid. Although **3** exists presumably as a mixture of four stereoisomers, the signals for the stereoisomers overlap within the resolution limits of both ^1H and ^{13}C NMR spectroscopic techniques. ^1H NMR (CD_3SOCD_3 , 500 MHz, 298 K): $\delta=12.96$ (s, 2H), 7.92 (s, 2H), 7.85 (d, $J=8.1$ Hz, 2H), 7.83 (AA'XX', $J=7.8$ Hz, 4H), 7.81–7.74 (AA'BB', 8H), 7.61 (d, $J=8.4$ Hz, 2H), 7.52 (AA'XX', $J=7.8$ Hz, 4H), 7.41 (d, $J=7.8$ Hz, 2H), 7.20 (dd, $J=8.0, 8.0$ Hz, 2H), 7.06 (s, 2H), 6.67 (d, $J=7.7$ Hz, 2H), 4.14–3.98 (m, 8H), 3.85–3.65 (m, 8H), 3.65–3.52 (m, 16H), 2.37 ppm (s, 6H); ^{13}C NMR (CD_3CN , 125 MHz, 298 K): 167.3, 153.8, 149.8, 145.2, 139.4, 139.0, 138.0, 137.0, 135.4, 131.4, 130.1, 129.9, 129.7, 129.6, 129.1, 127.0, 126.5, 126.2, 125.9, 125.3, 115.3, 113.8, 105.7, 70.2, 70.1, 70.1, 70.0, 69.1, 68.8, 68.4, 67.7, 20.3 ppm; HR MS (ESI): m/z calcd for $\text{C}_{72}\text{H}_{70}\text{O}_{14}$: 1158.4766 $[M]^+$; found: 1158.4750.

Synthesis of compound 12-4PF₆: Macrocylic polyether **9** (0.77 g, 0.61 mmol), **10-2PF₆**^[15] (0.87 g, 1.2 mmol), and α, α' -dibromo-*p*-xylene (0.32 g, 1.2 mmol) were dissolved in DMF (40 mL). The reaction mixture was stirred for 3 d at RT. The mixture was then poured directly onto a silica gel column and flushed with $(\text{CH}_3)_2\text{CO}$ to remove any remaining uncharged compounds. The column was then eluted with $\text{NH}_4\text{PF}_6/(\text{CH}_3)_2\text{CO}$ (0.10 mg/100 mL) to yield **12-4PF₆** (1.3 g, 90%) as a purple solid after counterion exchange with NH_4PF_6 . Although **12-4PF₆** exists presumably as a mixture of four stereoisomers, the signals for the stereoisomers overlap within the resolution limits of both ^1H and ^{13}C NMR spectroscopic techniques. ^1H NMR (CD_3CN , 500 MHz, 298 K): $\delta=9.18$ (AA'XX', $J=6.5$ Hz, 2H), 8.77 (AA'XX', $J=6.7$ Hz, 2H), 8.56 (AA'XX', $J=6.4$ Hz, 2H), 8.51 (AA'XX', $J=6.7$ Hz, 2H), 8.06–7.98 (m, 4H), 7.97 (br s, 2H), 7.91 (br s, 4H), 7.89 (AA'XX', $J=7.5$ Hz, 2H), 7.87 (AA'XX', $J=8.3$ Hz, 4H), 7.81 (AA'XX', $J=8.3$ Hz, 4H), 7.58 (AA'XX', $J=7.9$ Hz, 4H), 7.56 (AA'XX', $J=7.9$ Hz, 4H), 7.41 (AA'XX', $J=7.8$ Hz, 2H), 7.25 (AA'XX', $J=5.2$ Hz, 2H), 7.19 (AA'XX', $J=6.8, 2.4$ Hz, 2H), 6.90 (AA'XX', $J=6.7, 2.4$ Hz, 2H), 6.82 (AA'XX', $J=5.9$ Hz, 2H), 6.34 (s, 2H), 6.13 (d, $J=7.8$ Hz, 2H), 5.95–5.87 (m, 4H), 5.75–5.61 (m, 6H), 4.28–4.15 (m, 6H), 4.11–4.03 (m, 2H), 4.00–3.68 (m, 20H), 3.59 (t, $J=10.1$ Hz, 2H), 3.16 (br s, 2H), 2.41 (s, 6H), 2.34 (d, $J=8.1$ Hz, 2H), 1.62 ppm (s, 18H); ^{13}C NMR (CD_3CN , 125 MHz, 298 K): $\delta=166.3, 151.7, 150.0, 146.3, 145.8, 145.8, 145.2, 144.6, 144.3, 141.2, 140.1, 140.0, 137.5, 137.4, 136.8, 136.6, 132.6, 132.1, 132.0, 130.8, 130.7, 130.6, 129.1, 129.0, 127.7, 127.6, 127.4, 126.7, 127.4, 126.7, 125.6, 125.3, 125.1, 124.5, 115.0, 109.2, 105.0, 81.8, 72.1, 71.9, 70.6, 70.5, 70.3, 68.9, 68.9, 66.0, 28.3, 20.7$ ppm; HR MS (ESI): m/z calcd for $\text{C}_{116}\text{H}_{118}\text{F}_{24}\text{N}_4\text{O}_{14}\text{P}_4$: 1040.3959 $[M-2\text{PF}_6]^{2+}$; found: 1040.4001.

Synthesis of compound 1-4PF₆: Conc. HCl (30 mL) was added to a mixture of the catenane **12-4PF₆** (0.43 g, 0.18 mmol) and CH_3CN (40 mL). The reaction mixture was stirred for 30 min at RT, during which time a purple precipitate formed. The precipitate was collected by filtration, dissolved in H_2O with the assistance of a small amount of CH_3OH , and **1-4PF₆** (395 mg, 97%) was precipitated out of the solution as a purple solid with the addition of NH_4PF_6 . Although **1-4PF₆** exists presumably as a mixture of four stereoisomers, the signals for the stereoisomers overlap within the resolution limits of both ^1H and ^{13}C NMR spectroscopic techniques. ^1H NMR (CD_3CN , 500 MHz, 298 K): $\delta=9.21$ (AA'XX', $J=6.2$ Hz, 2H), 8.81 (AA'XX', $J=6.6$ Hz, 2H), 8.59 (AA'XX', $J=6.4$ Hz, 2H), 8.55 (AA'XX', $J=6.7$ Hz, 2H), 8.04 (m, 4H), 8.02 (br s, 2H), 7.94 (AA'XX', 8.0, 1.8 Hz, 2H), 7.91 (br s, 4H), 7.88 (AA'XX', $J=8.1$ Hz, 4H), 7.81 (AA'XX', $J=8.2$ Hz, 4H), 7.58 (AA'XX', $J=8.0$ Hz, 4H), 7.57

(AA'XX', $J=8.0$ Hz, 4H), 7.44 (AA'XX', $J=7.8$ Hz, 2H), 7.24 (AA'XX', $J=5.5$ Hz, 2H), 7.18 (AA'XX', $J=6.8, 2.4$ Hz, 2H), 6.89 (AA'XX', $J=6.6, 2.3$ Hz, 2H), 6.82 (AA'XX', $J=5.4$ Hz, 2H), 6.34 (s, 2H), 6.13 (d, $J=7.8$ Hz, 2H), 5.98–5.90 (m, 4H), 5.77–5.64 (m, 6H), 4.30–4.17 (m, 6H), 4.14–4.07 (m, 2H), 4.02–3.71 (m, 20H), 3.63 (t, $J=9.6$ Hz, 2H), 3.19 (br, 2H), 2.45 (s, 6H), 2.37 ppm (d, $J=8.1$ Hz, 2H); ^{13}C NMR (CD_3CN , 125 MHz, 298 K): $\delta=167.9, 151.9, 150.6, 150.1, 146.9, 146.3, 145.9, 145.3, 144.7, 141.3, 140.2, 140.1, 137.6, 137.5, 136.9, 132.6, 132.0, 131.0, 130.9, 130.7, 130.3, 129.2, 129.1, 128.2, 127.7, 127.6, 126.8, 125.7, 125.4, 125.2, 124.6, 115.1, 109.3, 105.1, 72.2, 72.1, 71.7, 70.6, 70.4, 69.1, 69.0, 66.0, 20.8$ ppm; HR MS (ESI): m/z calcd for $\text{C}_{108}\text{H}_{102}\text{F}_{24}\text{N}_4\text{O}_{14}\text{P}_4$: 984.3333 $[M-2\text{PF}_6]^{2+}$; found: 984.3343.

Synthesis of compound 13-4PF₆: A mixture of macrocyclic polyether **9** (0.450 g, 0.354 mmol), 2,7-diazapyrene **14**^[16] (0.216 g, 1.06 mmol), **11-2PF₆**^[17] (0.863 g, 1.06 mmol), and DMF (20 mL) was stirred at RT under N_2 for 7 d before the solvent was removed under vacuum. The solid residue was purified by column chromatography on silica gel using $(\text{CH}_3)_2\text{CO}$ and $\text{NH}_4\text{PF}_6/(\text{CH}_3)_2\text{CO}$ (0.25 g/100 mL to 1.5 g/100 mL) as the eluents. The fractions containing the product were combined, concentrated to a small volume, and an excess of H_2O was added to precipitate the product, which was then collected by filtration and washed several times with H_2O . After drying in air overnight, the pure product **13-4PF₆** (0.72 g, 84%) was obtained as a red-purple solid. In solution, **13-4PF₆** exists as a 3:1 (by ^1H NMR spectroscopy) mixture of two translational isomers (major-**13-4PF₆** and minor-**13-4PF₆**). Both major-**13-4PF₆** and minor-**13-4PF₆** exist presumably as a mixture of four stereoisomers, resulting in complex NMR spectra for **13-4PF₆**. Most of the ^1H and ^{13}C NMR signals of minor-**13-4PF₆** overlap with the signals of major-**13-4PF₆** or are broadened, but some individual ^1H NMR signals of minor-**13-4PF₆** can be identified. The ^1H and ^{13}C NMR signals of minor-**13-4PF₆** could not be fully assigned. Only the ^1H and ^{13}C NMR spectra of major-**13-4PF₆** are reported (the signals of the stereoisomers of major-**13-4PF₆** overlap within the resolution limits of both NMR spectroscopic techniques). Major-**13-4PF₆**: ^1H NMR (CD_3CN , 500 MHz, 298 K): $\delta=10.04$ (s, 2H), 9.43 (s, 2H), 8.56 (AA'XX', $J=6.6$ Hz, 2H), 8.51 (AA'XX', $J=6.4$ Hz, 2H), 8.19–8.13 (m, 2H), 8.09 (dd, $J=8.3, 1.9$ Hz, 2H), 7.98 (d, $J=1.7$ Hz, 2H), 7.98–7.93 (m, 4H), 7.92–7.84 (m, 2H), 7.90 (AA'XX', $J=8.0$ Hz, 4H), 7.87 (d, $J=9.5$ Hz, 2H), 7.79 (AA'XX', $J=8.2$ Hz, 4H), 7.65 (d, $J=9.2$ Hz, 2H), 7.57 (AA'XX', $J=8.0$ Hz, 4H), 7.42 (AA'XX', $J=8.3$ Hz, 4H), 7.42 (d, $J=8.1$ Hz, 2H), 7.12 (AA'XX', $J=6.7, 2.4$ Hz, 2H), 6.91 (AA'XX', $J=6.8, 2.4$ Hz, 2H), 6.44 (d, $J=13.7$ Hz, 2H), 6.10 (AA'XX', $J=13.8$ Hz, 2H), 5.73 (d, $J=7.9$ Hz, 2H), 5.70 (s, 2H), 5.65–5.62 (m, 4H), 5.60 (dd, $J=7.9, 7.9$ Hz, 2H), 4.44–4.36 (m, 2H), 4.35–4.26 (m, 4H), 4.14–3.62 (m, 22H), 3.60–3.49 (m, 4H), 2.43 (s, 6H), 1.76 (d, $J=8.3$ Hz, 2H), 1.63 ppm (s, 18H); ^{13}C NMR (CD_3CN , 125 MHz, 298 K): $\delta=166.4, 151.0, 149.4, 146.6, 145.9, 145.6, 143.8, 142.3, 141.3, 140.2, 140.2, 139.9, 137.6, 137.4, 136.7, 136.3, 132.1, 132.1, 132.0, 130.9, 130.8, 130.7, 130.7, 130.3, 130.1, 129.2, 128.6, 128.5, 127.9, 127.7, 127.6, 127.4, 127.1, 126.8, 125.7, 124.5, 123.2, 113.6, 107.2, 105.0, 81.8, 73.0, 72.9, 72.5, 71.1, 70.8, 70.4, 68.9, 68.9, 67.9, 66.1, 28.4, 20.8$ ppm; HRMS (ESI): m/z calcd for $\text{C}_{120}\text{H}_{118}\text{F}_{24}\text{N}_4\text{O}_{14}\text{P}_4$: 1064.3959 $[M-2\text{PF}_6]^{2+}$; found: 1064.3914.

Synthesis of compound 2-4PF₆: A mixture of **13-4PF₆** (118 mg, 48.8 μmol), TFA (13 mL), and CH_3CN (13 mL) was stirred at RT in the dark for 3 d before the solvents were evaporated. After the addition a 3:2 mixture of H_2O and CH_3OH (50 mL) followed by aq. NH_4PF_6 (1.5 M, 30 mL), the red precipitate that formed was collected by filtration, washed with H_2O , and dried in air to afford the pure product **2-4PF₆** (102 mg, 90%) as a dark red solid. In solution, **2-4PF₆** exists as a 3:1 (by ^1H NMR spectroscopy) mixture of two translational isomers (major-**2-4PF₆** and minor-**2-4PF₆**). Both major-**2-4PF₆** and minor-**2-4PF₆** exist presumably as a mixture of four stereoisomers, which results in complex NMR spectra for **2-4PF₆**. Most of the ^1H and ^{13}C NMR signals of minor-**2-4PF₆** overlap with the signals of major-**2-4PF₆** or are broadened, but some individual ^1H NMR signals of minor-**2-4PF₆** can be identified (Figure S4 in the Supporting Information). The ^1H and ^{13}C NMR signals of minor-**2-4PF₆** could not be fully assigned. Only the ^1H and ^{13}C NMR spectra of major-**2-4PF₆** are reported (the signals of the stereoisomers of major-**2-4PF₆** overlap within the resolution limits of both NMR spectroscopic techniques). Major-**2-4PF₆**: ^1H NMR (CD_3CN , 500 MHz, 298 K):

δ = 10.03 (s, 2H), 9.43 (s, 2H), 8.57 (AA'XX', J = 6.7 Hz, 2H), 8.51 (AA'XX', J = 6.5 Hz, 2H), 8.16 (dd, J = 8.4, 1.9 Hz, 2H), 8.08 (dd, J = 8.2, 1.9 Hz, 2H), 8.02 (d, J = 2.1 Hz, 2H), 7.98–7.88 (m, 6H), 7.91 (AA'XX', J = 8.1 Hz, 4H), 7.86 (d, J = 9.0 Hz, 2H), 7.79 (AA'XX', J = 8.3 Hz, 4H), 7.64 (d, J = 9.1 Hz, 2H), 7.58 (AA'XX', J = 8.0 Hz, 4H), 7.45 (d, J = 7.9 Hz, 2H), 7.43 (AA'XX', J = 8.5 Hz, 4H), 7.12 (AA'XX', J = 6.5, 2.4 Hz, 2H), 6.91 (AA'XX', J = 6.8, 2.4 Hz, 2H), 6.44 (d, J = 13.7 Hz, 2H), 6.10 (d, J = 13.7 Hz, 2H), 5.72 (d, J = 7.9 Hz, 2H), 5.70 (s, 2H), 5.65–5.62 (m, 4H), 5.60 (dd, J = 8.0, 7.9 Hz, 2H), 4.44–4.36 (m, 2H), 4.35–4.26 (m, 4H), 4.14–3.62 (m, 22H), 3.60–3.49 (m, 4H), 2.44 (s, 6H), 1.76 ppm (d, J = 8.0 Hz, 2H); ^{13}C NMR (CD_3CN , 125 MHz, 298 K): δ = 167.7, 151.0, 149.4, 147.0, 145.9, 145.6, 143.9, 142.3, 141.2, 140.3, 140.2, 139.8, 137.6, 137.4, 136.9, 136.3, 132.6, 132.6, 132.0, 131.0, 130.9, 130.7, 130.7, 130.3, 130.1, 129.2, 128.6, 128.2, 127.9, 127.8, 127.7, 127.6, 127.4, 127.2, 126.8, 125.7, 124.5, 123.2, 113.6, 107.2, 105.0, 73.0, 72.9, 72.5, 71.1, 70.8, 70.4, 68.9, 68.9, 67.9, 66.1, 20.8 ppm; HRMS (ESI): m/z calcd for $\text{C}_{112}\text{H}_{102}\text{F}_{24}\text{N}_4\text{O}_{14}\text{P}_4$: 1008.3333 [$M-2\text{PF}_6$] $^{2+}$; found: 1008.3307.

Synthesis of compound MOF-1050: $\text{Cu}(\text{NO}_3)_2 \cdot 2.5\text{H}_2\text{O}$ (20 mg, 86 μmol) and **1-4PF₆** (10 mg, 4.4 μmol) were dissolved in a 3:3:2 (v/v/v) mixture (1 mL) of DEF, EtOH, and H_2O . The mixture was passed through a 0.45 μm filter into a 3 mL vial which was capped and heated in an isothermal oven at 85 °C for 3 d, after which time it was removed from the oven and cooled to room temperature, yielding a mixture of brown and green crystals. The brown crystals of $[\text{Cu}_2(\mathbf{1})_2(\text{H}_2\text{O})_2]$ (MOF-1050) were characterized^[24] by single-crystal X-ray crystallography.^[23]

Synthesis of compound MOF-1051: $\text{Cu}(\text{NO}_3)_2 \cdot 2.5\text{H}_2\text{O}$ (3.9 mg, 17 μmol) and **2-4PF₆** (2.0 mg, 0.87 μmol) were dissolved in a 3:3:2 (v/v/v) mixture (1 mL) of DEF, EtOH, and H_2O . The mixture was passed through a 0.45 μm filter equally into three 1 mL crystallization tubes which were capped in a 20 mL vial and heated in an isothermal oven at 80 °C for 2 d, after which time they were removed from the oven and cooled to room temperature, yielding a mixture of orange and green crystals. The orange crystals of $[\text{Cu}_2(\mathbf{2})_2(\text{H}_2\text{O})_2]$ (MOF-1051) were characterized^[25] by single-crystal X-ray crystallography.^[23]

MOF-1052: $\text{Cu}(\text{NO}_3)_2 \cdot 2.5\text{H}_2\text{O}$ (3.9 mg, 17 μmol) and **3** (1.0 mg, 0.79 μmol) were dissolved in a 3:3:2 (v/v/v) mixture (1 mL) of DMF, EtOH, and H_2O . The mixture was passed through a 0.45 μm filter equally into three 1 mL crystallization tubes which were capped in a 20 mL vial and heated in an isothermal oven at 60 °C for 5 d, after which time they were removed from the oven and cooled to room temperature, yielding a mixture of blue and green crystals. The blue crystals of $[\text{Cu}(\mathbf{3})(\text{H}_2\text{O})_2(\text{dmf})]$ (MOF-1052) were characterized^[31] by single-crystal X-ray crystallography.^[23]

Acknowledgements

D.C. acknowledges the National Science Foundation (NSF) for a Graduate Research Fellowship. D.C. and J.F.S. were beneficiaries of the WCU Program funded by the Ministry of Education, Science and Technology, Korea (NRF R-31-2008-000-10055-0). D.C. gratefully acknowledges support from the Ryan Fellowship and the Northwestern University International Institute for Nanotechnology. M.J. gratefully acknowledges the Netherlands Organisation for Scientific Research (NWO) and the Marie Curie Cofund Action (Rubicon Fellowship) for financial support. S.G. gratefully acknowledges the Swiss National Science Foundation for financial support. Z.J.B., J.T.H., and O.K.F. gratefully acknowledge financial support from the Defense Threat Reduction Agency (grant Nos. HDTRA1-09-1-0007 and HDTRA1-1-10-0023).

- [1] a) Q. Li, W. Zhang, O. Š. Miljanić, C.-H. Sue, C. B. Knobler, Y.-L. Zhao, L. Liu, J. F. Stoddart, O. M. Yaghi, *Science* **2009**, *325*, 855–859; b) C. Valente, E. Choi, M. E. Belowich, C. J. Doonan, T. B. Gasa, Y. Y. Botros, O. M. Yaghi, J. F. Stoddart, *Chem. Commun.* **2010**, *46*, 4911–4913; c) N. L. Strutt, D. Fairen-Jimenez, J. Jehl,

- M. B. LaLonde, R. Q. Snurr, O. K. Farha, J. T. Hupp, J. F. Stoddart, *J. Am. Chem. Soc.* **2012**, *134*, 17436–17439.
- [2] a) G. Schill, *Catenanes, Rotaxanes, and Knots*, Academic Press, New York, **1971**; b) *Molecular Catenanes, Rotaxanes, and Knots* (Eds.: J.-P. Sauvage, C. Dietrich-Buchecker), Wiley-VCH, Weinheim, **1999**; c) D. B. Amabilino, J. F. Stoddart, *Chem. Rev.* **1995**, *95*, 2725–2828; d) M. Fujita, *Acc. Chem. Res.* **1999**, *32*, 53–61; e) L. Raehm, D. G. Hamilton, J. K. M. Sanders, *Synlett* **2002**, 1743–1761; f) K. Kim, *Chem. Soc. Rev.* **2002**, *31*, 96–107; g) J. F. Stoddart, *Chem. Soc. Rev.* **2009**, *38*, 1802–1820; h) J. E. Beves, B. A. Blight, C. J. Campbell, D. A. Leigh, R. T. McBurney, *Angew. Chem.* **2011**, *123*, 9428–9499; *Angew. Chem. Int. Ed.* **2011**, *50*, 9260–9327; i) R. S. Forgan, J.-P. Sauvage, J. F. Stoddart, *Chem. Rev.* **2011**, *111*, 5434–5464.
- [3] a) H. Li, M. Eddaoudi, M. O'Keefe, O. M. Yaghi, *Nature* **1999**, *402*, 276–279; b) S. L. James, *Chem. Soc. Rev.* **2003**, *32*, 276–288; c) S. Kitagawa, R. Kitaura, S. Noro, *Angew. Chem.* **2004**, *116*, 2388–2430; *Angew. Chem. Int. Ed.* **2004**, *43*, 2334–2375; d) R. J. Hill, D.-L. Long, N. R. Champness, P. Hubberstey, M. Schröder, *Acc. Chem. Res.* **2005**, *38*, 335–348; e) G. Férey, *Chem. Soc. Rev.* **2008**, *37*, 191–241; f) J. R. Long, O. M. Yaghi, *Chem. Soc. Rev.* **2009**, *38*, 1213–1214; g) T. R. Cook, Y.-R. Zheng, P. J. Stang, *Chem. Rev.* **2013**, *113*, 734–777.
- [4] a) E. Lee, J. Kim, J. Heo, D. Whang, K. Kim, *Angew. Chem.* **2001**, *113*, 413–416; *Angew. Chem. Int. Ed.* **2001**, *40*, 399–402; b) V. N. Vukotic, S. J. Loeb, *Chem. Eur. J.* **2010**, *16*, 13630–13637; c) H.-Y. Gong, B. M. Rambo, W. Cho, V. M. Lynch, M. Oh, J. L. Sessler, *Chem. Commun.* **2011**, 47, 5973–5975; d) V. N. Vukotic, K. J. Harris, K. Zhu, R. W. Schurko, S. J. Loeb, *Nat. Chem.* **2012**, *4*, 456–460; e) A. Coskun, M. Hmadeh, G. Barin, F. Gandara, Q. Li, E. Choi, N. L. Strutt, D. B. Cordes, A. M. Z. Slawin, J. F. Stoddart, *Angew. Chem.* **2012**, *124*, 2202–2205; *Angew. Chem. Int. Ed.* **2012**, *51*, 2160–2163.
- [5] a) G. J. E. Davidson, S. J. Loeb, *Angew. Chem.* **2003**, *115*, 78–81; *Angew. Chem. Int. Ed.* **2003**, *42*, 74–77; b) D. J. Hoffart, S. J. Loeb, *Angew. Chem.* **2005**, *117*, 923–926; *Angew. Chem. Int. Ed.* **2005**, *44*, 901–904; c) S. J. Loeb, *Chem. Commun.* **2005**, 1511–1518; d) S. J. Loeb, *Chem. Soc. Rev.* **2007**, *36*, 226–235; e) V. N. Vukotic, S. J. Loeb, *Chem. Soc. Rev.* **2012**, *41*, 5896–5906.
- [6] H. Deng, M. A. Olson, J. F. Stoddart, O. M. Yaghi, *Nat. Chem.* **2010**, *2*, 439–443.
- [7] a) Q. Li, W. Zhang, O. Š. Miljanić, C. B. Knobler, J. F. Stoddart, O. M. Yaghi, *Chem. Commun.* **2010**, 46, 380–382; b) Q. Li, C.-H. Sue, S. Basu, A. K. Shveyd, W. Zhang, G. Barin, L. Fang, A. A. Sarjeant, J. F. Stoddart, O. M. Yaghi, *Angew. Chem.* **2010**, *122*, 6903–6907; *Angew. Chem. Int. Ed.* **2010**, *49*, 6751–6755.
- [8] Recently, we introduced molecular gauge blocks based on 1–7 and 9–11 paraxylene rings as part of a homologous series of oligoparaxylenes with a view to providing a molecular tool box for the construction of extended structures such as metal–organic frameworks; see: S. Grunder, C. Valente, A. C. Whalley, S. Sampath, J. Portmann, Y. Y. Botros, J. F. Stoddart, *Chem. Eur. J.* **2012**, *18*, 15632–15649. These molecular gauge blocks have been incorporated into an isorecticular series of MOF-74 structures with pore apertures ranging from 14 to 98 Å; see: H. Deng, S. Grunder, K. E. Cordova, C. Valente, H. Furukawa, M. Hmadeh, F. Gándara, A. C. Whalley, Z. Liu, S. Asahira, H. Kazumorio, M. O'Keefe, O. Terasake, J. F. Stoddart, O. M. Yaghi, *Science* **2012**, *336*, 1018–1023.
- [9] The square paddlewheel is one of the most common clusters formed between metal ions and carboxylates; see the following and references therein: D. J. Tranchemontagne, J. L. Mendoza-Cortés, M. O'Keefe, O. M. Yaghi, *Chem. Soc. Rev.* **2009**, *38*, 1257–1283. The axial positions of the paddlewheels can be coordinated to a large variety of ligands—typically, solvent molecules, such as H_2O and DMF, are present in freshly synthesized MOFs. Desolvating the paddlewheels yields open metal sites which have been exploited for enhanced gas adsorption properties of the crystalline materials; see: a) M. Dincă, J. R. Long, *Angew. Chem.* **2008**, *120*, 6870–6884; *Angew. Chem. Int. Ed.* **2008**, *47*, 6766–6779; b) Y. Yan, I. Telepeni, S. Yang, X. Lin, W. Kockelmann, A. Dailly, A. J. Blake, W. Lewis,

- G. S. Walker, D. R. Allan, S. A. Barnett, N. R. Champness, M. Schröder, *J. Am. Chem. Soc.* **2010**, *132*, 4092–4094.
- [10] For a review on the nature of $\pi\cdots\pi$ interactions in self-assembly processes, see: C. G. Claessens, J. F. Stoddart, *J. Phys. Org. Chem.* **1997**, *10*, 245–272. For an earlier general discussion on $\pi\cdots\pi$ stacking interactions, see C. A. Hunter, J. K. M. Sanders, *J. Am. Chem. Soc.* **1990**, *112*, 5525–5534. For a recent general discussion, see: C. R. Martinez, B. L. Iverson, *Chem. Sci.* **2012**, *3*, 2191–2201.
- [11] Syndiotactic polymer chains, which are characterized by alternating stereocenters, often exhibit properties not found in their atactic partners; see a) E. L. Eliel, *Stereochemistry of Carbon Compounds*, McGraw-Hill, New York, **1962**; b) P. C. Hiemenz, T. P. Lodge, in *Polymer Chemistry*, 2nd ed., CRC, Boca Raton, **2007**.
- [12] T. Ishiyama, M. Murata, N. Miyaura, *J. Org. Chem.* **1995**, *60*, 7508–7510.
- [13] N. Miyaura, K. Yamada, A. Suzuki, *Tetrahedron Lett.* **1979**, *20*, 3437–3440.
- [14] Y.-L. Zhao, L. Liu, W. Zhang, C.-H. Sue, Q. Li, O. Š. Miljanić, O. M. Yaghi, J. F. Stoddart, *Chem. Eur. J.* **2009**, *15*, 13356–13380.
- [15] B. Odell, M. V. Reddington, A. M. Z. Slawin, N. Spencer, J. F. Stoddart, D. J. Williams, *Angew. Chem.* **1988**, *100*, 1605–1608; *Angew. Chem. Int. Ed. Engl.* **1988**, *27*, 1547–1550.
- [16] A. J. Blake, G. Baum, N. R. Champness, S. S. M. Chung, P. A. Cooke, D. Fenske, A. N. Khlobystov, D. A. Lemenovskii, W.-S. Li, M. Schröder, *J. Chem. Soc. Dalton Trans.* **2000**, 4285–4291.
- [17] D. J. Williams, P. R. Ashton, R. Ballardini, V. Balzani, A. Credi, M. T. Gandolfi, S. Menzer, L. Pérez-García, L. Prodi, J. F. Stoddart, M. Venturi, A. J. P. White, *J. Am. Chem. Soc.* **1995**, *117*, 11171–11197.
- [18] P. S. Kalsi, *Stereochemistry Conformation and Mechanism*, 6th ed., New Age International, New Delhi, **2005**.
- [19] R. S. Cahn, C. Ingold, V. Prelog, *Angew. Chem.* **1966**, *78*, 413–447; *Angew. Chem. Int. Ed. Engl.* **1966**, *5*, 385–415.
- [20] S. A. Vignon, J. F. Stoddart, *Collect. Czech. Chem. Commun.* **2005**, *70*, 1493–1576.
- [21] A similar ratio of translational isomers was observed in an analogous [2]catenane without pendant terphenylene units; see: P. R. Ashton, S. E. Boyd, A. Brindle, S. J. Langford, S. Menzer, L. Pérez-García, J. A. Preece, F. M. Raymo, N. Spencer, J. F. Stoddart, A. J. P. White, D. J. Williams, *New J. Chem.* **1999**, *23*, 587–602.
- [22] The use of an excess of $\text{Cu}(\text{NO}_3)_2 \cdot 2.5\text{H}_2\text{O}$ during the production of MOF-1050 and MOF-1051 ensures that all the PF_6^- counterions are exchanged for the NO_3^- counterions.
- [23] CCDC-913139 (MOF-1050), CCDC-913140 (MOF-1051), and CCDC-913141 (MOF-1052) contain the supplementary crystallographic data for this paper. These data can be obtained free of charge from The Cambridge Crystallographic Data Centre via www.ccdc.cam.ac.uk/data_request/cif.
- [24] Crystal data for MOF-1050: $\text{C}_{108}\text{H}_{100}\text{CuN}_4\text{O}_{15}$, $M_r = 1757.46 \text{ g mol}^{-1}$, monoclinic, space group $P2_1/n$ (no. 14), $a = 12.7797(5)$, $b = 49.577(2)$, $c = 26.7601(10) \text{ \AA}$, $\alpha = 90.00^\circ$, $\beta = 100.039(2)$, $\gamma = 90.00^\circ$, $V = 16695.1(11) \text{ \AA}^3$, $\rho_{\text{calcd}} = 0.699 \text{ g cm}^{-3}$, $\mu(\text{Cu}_{\text{K}\alpha}) = 0.491 \text{ mm}^{-1}$, $T = 224.98 \text{ K}$, brown blocks, 79708 measured reflections, F^2 refinement, $R_1 = 0.2113$, $wR_2 = 0.4377$, 17384 independent observed reflections (all data), 1155 parameters.
- [25] Crystal data for MOF-1051: $\text{C}_{112}\text{H}_{100}\text{CuN}_4\text{O}_{15}$, $M_r = 1805.50 \text{ g mol}^{-1}$, monoclinic, space group $P2_1/n$ (no. 14), $a = 12.6962(6)$, $b = 48.752(2)$, $c = 26.1253(12) \text{ \AA}$, $\alpha = 90.00^\circ$, $\beta = 100.219(4)$, $\gamma = 90.00^\circ$, $V = 15914.1(13) \text{ \AA}^3$, $\rho_{\text{calcd}} = 0.754 \text{ g cm}^{-3}$, $\mu(\text{Cu}_{\text{K}\alpha}) = 0.524 \text{ mm}^{-1}$, $T = 99.99 \text{ K}$, orange blocks, 37477 measured reflections, F^2 refinement, $R_1 = 0.1993$, $wR_2 = 0.4207$, 7548 independent observed reflections (all data), 1189 parameters.
- [26] a) E. Alcalde, L. Pérez-García, S. Ramos, J. F. Stoddart, S. A. Vignon, A. J. P. White, D. J. Williams, *Mendeleev Commun.* **2003**, *13*, 100–102; b) E. Alcalde, L. Pérez-García, S. Ramos, J. F. Stoddart, S. A. Vignon, A. J. P. White, D. J. Williams, *Mendeleev Commun.* **2004**, *14*, 233–235.
- [27] a) H. Chun, D. Dybtsev, H. Kim, K. Kim, *Chem. Eur. J.* **2005**, *11*, 3521–3529; b) B.-Q. Ma, K. L. Mulfort, J. T. Hupp, *Inorg. Chem.* **2005**, *44*, 4912–4914.
- [28] The angle was measured between the plane of the HQ ring and the line from the centroid of the copper paddlewheel to the centroid of the HQ ring.
- [29] For an example of a [2]catenane whose solid-state structure exhibits crossed tetracationic cyclophanes within a single DA stack of catenanes, see: D. L. Simone, T. M. Swager, *J. Am. Chem. Soc.* **2000**, *122*, 9300–9301.
- [30] The porosity of MOF-1050 was examined by CO_2 adsorption at 273 K after the guest solvent molecules were removed using supercritical CO_2 , and found to be about $350 \text{ m}^2 \text{ g}^{-1}$ —the details of activation are located in the Supporting Information; also see: a) A. P. Nelson, O. K. Farha, K. L. Mulfort, J. T. Hupp, *J. Am. Chem. Soc.* **2009**, *131*, 458–460; b) O. K. Farha, J. T. Hupp, *Acc. Chem. Res.* **2010**, *43*, 1166–1175.
- [31] Crystal data for MOF-1052: $\text{C}_{153}\text{H}_{165}\text{Cu}_2\text{N}_3\text{O}_{35}$, $M_r = 2732.96 \text{ g mol}^{-1}$, triclinic, space group $P\bar{1}$ (no. 2), $a = 13.4730(3)$, $b = 20.6981(4)$, $c = 31.1920(6) \text{ \AA}$, $\alpha = 100.4170(10)$, $\beta = 100.8960(10)$, $\gamma = 108.7780(10)^\circ$, $V = 7808.9(3) \text{ \AA}^3$, $\rho_{\text{calcd}} = 1.162 \text{ g cm}^{-3}$, $\mu(\text{Cu}_{\text{K}\alpha}) = 0.921 \text{ mm}^{-1}$, $T = 224.99 \text{ K}$, blue blocks, 38206 measured reflections, F^2 refinement, $R_1 = 0.1138$, $wR_2 = 0.2664$, 24191 independent observed reflections (all data), 1811 parameters.
- [32] a) J. M. Lehn, *Supramolecular Chemistry*; Wiley-VCH, Weinheim, **1995**; b) J. F. Stoddart, *Nat. Chem.* **2009**, *1*, 14–15; c) J. M. Lehn, *Top. Curr. Chem.* **2012**, *322*, 1–32; d) J. F. Stoddart, *Angew. Chem.* **2012**, *124*, 13076–13077; *Angew. Chem. Int. Ed.* **2012**, *51*, 12902–12902.
- [33] a) B. J. Hathaway, G. Wilkinson, R. D. Gillard, *Comprehensive Coordination Chemistry*, Pergamon, Oxford, **1987**; b) B. J. Holliday, C. A. Mirkin, *Angew. Chem.* **2001**, *113*, 2076–2097; *Angew. Chem. Int. Ed.* **2001**, *40*, 2022–2043.
- [34] A. Coskun, J. M. Spruell, G. Barin, W. R. Dichtel, A. H. Flood, Y. Y. Botros, J. F. Stoddart, *Chem. Soc. Rev.* **2012**, *41*, 4827–4859.
- [35] A. Coskun, M. Banaszak, R. D. Astumian, J. F. Stoddart, B. A. Grzybowski, *Chem. Soc. Rev.* **2012**, *41*, 19–30.
- [36] M. A. Olson, Y. Y. Botros, J. F. Stoddart, *Pure Appl. Chem.* **2010**, *82*, 1569–1574.
- [37] T. Mineno, T. Ueno, Y. Urano, H. Kojima, T. Nagano, *Org. Lett.* **2006**, *8*, 5963–5966.

Received: February 26, 2013
Published online: May 6, 2013